

A pre-explosion extended effervescent zone around core collapse supernova progenitors

NOAM SOKER^{1,2}

¹*Department of Physics, Technion, Haifa, 3200003, Israel; soker@physics.technion.ac.il*

²*Guangdong Technion Israel Institute of Technology, Shantou 515069, Guangdong Province, China*

ABSTRACT

I propose a scenario according to which the dense compact circumstellar matter (CSM) that the ejecta of many core collapse supernovae (CCSNe) collide with within several days after explosion results from a dense zone where in addition to the stellar wind there is gas that does not reach the escape velocity. In this effervescent zone around red supergiant (RSG) stars, there are dense clumps that are ejected from the vicinity of the RSG surface, rise to radii of tens of astronomical units, and then fall back. I consider two simple velocity distributions of the ejected clumps. I find that the density of the bound mass can be tens of times that of the escaping wind, and therefore can mimic a very high mass loss rate. The dense effervescent compact CSM zone can (1) explain the collision of the ejecta of many CCSNe with a dense compact CSM days after explosion, (2) facilitate very high mass loss rate if the star experiences powerful pre-explosion activity, (3) form dust that obscures the progenitor in the visible band, and (4) lead to an efficient mass transfer to a stellar companion at separations of tens of astronomical units, if exists. The effervescent zone might exist for thousands of years and more, and therefore the effervescent CSM model removes the requirement from many type II CCSN progenitors to experience a very strong outburst just years to months before explosion.

Keywords: stars: massive – stars: mass-loss – supernovae: general

1. INTRODUCTION

There are two types of indications to the presence of compact circumstellar matter (CSM) around many, but not all, progenitors of core collapse supernovae (CCSNe) at explosion. One indication comes from pre-explosion outbursts years to months before the explosion and the other is the collision of the CCSN ejecta with compact CSM.

CCSNe are the explosions of stars that leave behind either a neutron star or a black hole. Stars in the initial mass range of $\gtrsim 10M_{\odot}$ form an iron core at the end of their nuclear burning phases. When the mass of the iron core grows to about $1.2M_{\odot}$ the core collapses to form a NS (or with more mass a black hole). A small fraction of the gravitational energy that the formation of the neutron star releases explodes the rest of the star. Stars in the initial mass range of $\simeq 8M_{\odot}$ to $\simeq 10M_{\odot}$ might collapse at an earlier phase, when their core is made up from ONeMg. Electron capture by magnesium in the degenerate core reduces the pressure and leads to core collapse, leaving behind a neutron star. In this study I consider the compact CSM around red supergiant (RSG) progenitors of both types of core collapse.

Pre-explosion outbursts that are accompanied by high mass loss rate episodes might occur tens of years to only days prior to explosion (e.g., Foley et al. 2007; Pastorello et al. 2007; Smith et al. 2010; Pastorello et al. 2013; Margutti et al. 2014; Ofek et al. 2014; Svirski & Nakar 2014; Tartaglia et al. 2016; Strotjohann et al. 2021). In some cases the pre-explosion outburst might take place as early as carbon-burning phase (e.g., Moriya et al. 2014; Margutti et al. 2017).

Yaron et al. (2017) argue that the progenitor of SN 2013fs had an enhanced mass loss rate of $\simeq 0.3 - 4 \times 10^{-3}M_{\odot} \text{ yr}^{-1}$ for a wind velocity of $v_w \approx 15 - 100 \text{ km s}^{-1}$. They find the wind velocity to be $v_w \lesssim 100 \text{ km s}^{-1}$. Hosseinzadeh et al. (2018) estimate the mass of the compact CSM around the progenitor of SN 2016bkv to be $\approx 0.04M_{\odot}$. The typical sizes of the compact CSM that, e.g., Bruch et al. (2020), find around CCSNe, on the other hand, are $R_{\text{CSM}} \approx 10^{15} \text{ cm}$. If this compact CSM is an outflowing wind, the high mass loss rate begins at about $\simeq R_{\text{CSM}}/v_w \approx 3 \text{ yr}$, where $v_w \simeq 100 \text{ km s}^{-1}$ is the wind velocity. In some cases the pre-explosion wind starts only several months before explosion (e.g., Bruch et al. 2020). Prentice et al. (2020) claim that the CSM around the envelope-stripped SN 2018gix was ejected within four months

from explosion. In that case the CSM is non-spherical, most likely indicating a pre-explosion binary interaction (Prentice et al. 2020).

There are theoretical studies that include an enhanced mass loss rate years to months before explosion as a result of core activity (e.g., Morozova et al. 2020), either set by excitation of waves (e.g., Quataert & Shiode 2012; Shiode & Quataert 2014; Fuller 2017; Fuller & Ro 2018) or by core-magnetic activity (e.g., Soker & Gilkis 2017). There are two problems with such a core activity as an explanation to all cases of SNe II with compact CSM. (1) In many cases this core activity might lead to substantial envelope expansion, but without much mass loss rate enhancement (e.g., Mcley & Soker 2014). (2) Bruch et al. (2020) find that $> 30\%$ of SNe II have compact CSM, while the fraction of CCSNe that suffer a pre-explosion outburst, which the core activity should excite, is only $\approx 10\%$ (e.g., Margutti et al. 2017).

Although pre-explosion outbursts do occur, in the present study I consider another model to account for the frequent presence of compact CSM, the *effervescent CSM model*. In this model there is a dense bound mass in an extended zone around the RSG surface (an extended zone relative to the stellar radius, but at the same time a compact CSM). Dessart et al. (2017) presented the idea of a long-lived complex extended dense zone around RSG progenitors of CCSNe that might have up to $\approx 0.01M_{\odot}$. There are some similarities between their model and the effervescent CSM model. Before presenting the effervescent CSM model for CCSN progenitors, I turn to describe the motivation for introducing this model.

In low-mass asymptotic giant branch (AGB) stars that are potential progenitors of planetary nebulae there are several observations that have led to the development of the effervescent CSM (wind) model (Soker 2008). These observations include complicated structures of SiO maser clumps (e.g., Cotton et al. 2006) and a chaotic inflow-outflow motion around the surface of some AGB stars (e.g., Diamond & Kemball 2003). Water maser observations that explore regions at larger distances from the surface of some AGB stars, $r \approx 100$ AU, also indicate inhomogeneous outflows (e.g., Vlemmings et al. 2002). The distribution of dust close to some AGB stars is also inhomogeneous, and might be related to the magnetic field in the atmosphere of AGB stars (e.g., Khouri et al. 2020 and references therein). Mira A is a pulsating AGB star with a radius of $R_1 \simeq 500R_{\odot}$ (e.g., Wood & Karovska 2006), and with an inhomogeneous and clumpy asymmetrical tens-AUs extended zone, that is, a compact CSM (e.g., Planesas et al. 1990; Ryde & Schöier 2001; Lopez et al. 1997). Lopez et al. (1997) con-

sidered a model where dusty clumps ≈ 100 times denser than their environment exist at tens of AUs from the AGB star Mira A. They assume these clumps to explain the IR emission, but did not consider the motion of the clumps.

The carbon AGB star IRC+10216 further motivates the introduction of the effervescent CSM model as it has clumps within ≈ 10 AU that Fonfría et al. (2008) suggest move outward and inward at high velocities along different radial directions; the fast outward moving clumps reaches distances of $\gg 10$ AU. The post-AGB star HD56126 has both outflowing and inflowing gas around it at velocities of up to $\simeq 20$ km s $^{-1}$ (Klochkova & Chentsov 2007). These velocities are non-negligible with respect to the escape velocity of $\simeq 60$ km s $^{-1}$ from this star (Li 2003).

More relevant to the present study are observations of inhomogeneous winds in RSGs (e.g., Lobel & Dupree 2000; Humphreys et al. 2007), including massive dust clumps around the RSG VY CMa (Kamiński 2019). Observations (e.g., Josselin & Plez 2007) and theoretical studies (e.g., Freytag et al. 2002) suggest that such inhomogeneous winds might result from convective cells in the envelope and/or magnetic activity of the giant stars. Boian & Groh (2020) argue that CCSNe with CSM tend to come from high mass RSGs, i.e., having zero age main sequence mass of $M_{ZAMS} \gtrsim 15M_{\odot}$. This also suggests luminous CCSN progenitors that can lift gas above the photosphere. There are studies of extended region where inflow and outflow coexist around stars that are close to their Eddington luminosity limit (e.g., Owocki & van Marle 2008; van Marle et al. 2009).

The above studies motivated me to introduce the effervescent CSM model to upper AGB stars (Soker 2008). The basic postulate of this model is that the zone up to about 100 AUs is inhomogeneous and contains many clumps that do not escape the star, but rather fall back.

Moriya et al. (2017) consider a dense compact CSM that results from the acceleration zone of the wind. Namely, instead of a constant wind velocity they consider a wind with a velocity that increases with radius, a profile that makes the density higher than of a constant-velocity wind very close to the stellar surface (also Moriya et al. 2018). The effervescent CSM model is different in some key aspects that I discuss later.

Dessart et al. (2017) simulate CCSN explosion inside an extended complex CSM that is bound or a dense wind. Numerically, they took either an atmosphere with an extended scale height and/or a dense wind. The effervescent CSM model share some properties and implications with their complex extended zone. They cite as motivation for considering such an extended zone

the observations of the RSG Betelgeuse that show outflows and inflows (down-flows) out to several RSG stellar radii (e.g., Ohnaka et al. 2011; Kervella et al. 2016). Dessart et al. (2017) noted that the extended zone removes the requirement for a fine-tuned stellar activity years to months before explosion. I also consider an extended zone, and in that I overlap with their study, but I consider the effervescent model of clumps that move out and fall back. I borrow the effervescent CSM model from low mass AGB progenitors of planetary nebulae. Nonetheless, I actually strengthen the claim of Dessart et al. (2017) that an extended zone around the photosphere of many RSG progenitors of CCSNe might explain observations.

In section 2 I present the basic condition for the presence of an effervescent CSM, and in section 3 I estimate the outer boundary of the effervescent zone. In section 4 I present one type of model for the effervescent zone and in section 5 I present another type. I summarise in section 6.

2. THE CONDITIONS FOR A DENSE EFFERVESCENT ZONE

Stellar pulsations, magnetic activity, rotation, and/or strong convection bring gas to the zone above and close to the photosphere. The stellar radiation cannot bring all this gas to escape, but brings a large fraction to almost escape velocities. This implies that the effervescent zone will be dense when the stellar radiation cannot accelerate most of the gas around the photosphere to escape velocity. In other words, the effervescent zone will become extended when the radiation momentum flux is about equal to the wind momentum flux. This might be the case during regular evolution of massive RSG stars, and more so for all RSG when powerful convection in the core (e.g., Quataert & Shiode 2012; Fuller 2017; Fuller & Ro 2018) and/or a powerful dynamo in the core (e.g., Soker & Gilkis 2017) drive stronger convection in the envelope. In turn, the stronger envelope convection pushes more gas above the photosphere. This process does not require the power of these activities to be more than what convection in the envelope can carry as the direct mass ejection mechanism requires. For that, this process of mass lifting can start when core activity is still weak, implying many years, even thousands of years and more, before the explosion. There is no need for a fine tuning of the activity to form the compact CSM.

At that stage when the radiation cannot accelerate most of the gas to the escape speed the mass loss rate in the wind is $\dot{M}_{wc} \simeq \eta_w L / (c v_w)$, where v_w is the terminal wind speed, L the stellar luminosity, and η_w is the average net effective times that a photon transfers

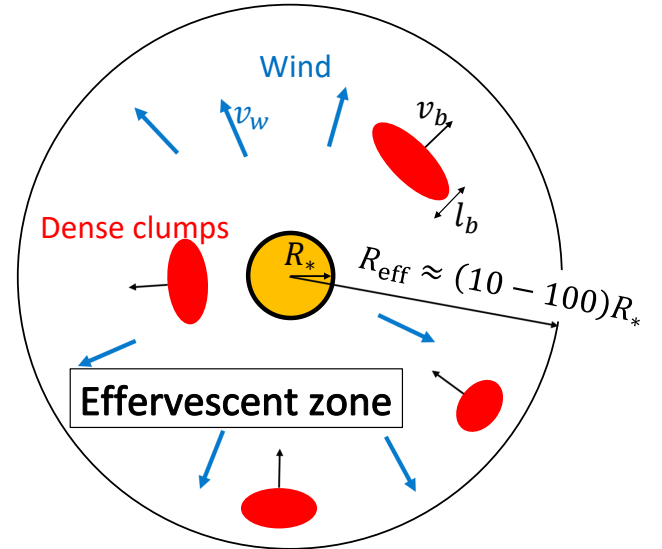


Figure 1. A schematic drawing of the effervescent zone (not to scale). The thick-blue arrows depict the escaping wind at its more than escape velocity v_w . The red-oval clouds depict the dense clumps that rise and fall within the effervescent zone. The orange sphere at the center is the RSG star of radius R_* . The outer edge of the effervescent zone is at R_{eff} .

momentum to the wind (only in the outward radial direction). In most cases $\eta_w < 1$, but in dense and opaque winds it can be somewhat larger than 1. Substituting typical values gives

$$\begin{aligned} \dot{M}_{wc} &\simeq 4 \times 10^{-5} \eta_w \left(\frac{L}{2 \times 10^5 L_\odot} \right) \\ &\times \left(\frac{v_w}{100 \text{ km s}^{-1}} \right)^{-1} M_\odot \text{ yr}^{-1}. \end{aligned} \quad (1)$$

This shows that the effervescent zone becomes significant when mass loss rate is high. But when we consider the effervescent zone, the mass loss rate into the wind need not be as high as estimates that do not consider the effervescent zone require.

3. A SINGLE CLUMP

Let us compare the different forces that act on a clump that is k_b times denser than the ambient wind density, $\rho_b = k_b \rho_w$, and it moves at radial distances of tens of AU, i.e., $r \gg R_*$, where R_* is the stellar radius. The wind density is $\rho_w = \dot{M}_w / 4\pi r^2 v_w$, where \dot{M}_w is the mass loss rate into the wind, and v_w the wind velocity. I further characterise the clump with its cross section facing the star (perpendicular to the radial direction) A_b and its length in the radial direction l_b . I schematically draw the effervescent zone in Figure 1.

The (radial) gravitational force on the clump due to the RSG star of mass M_* is

$$F_g = -\frac{GM_*}{r^2} \frac{\dot{M}_w}{4\pi r^2 v_w} k_b A_b l_b. \quad (2)$$

The regular wind exerts drag force on the clump. In this simple treatment I take this force to be

$$F_w \simeq \frac{\dot{M}_w v_w}{4\pi r^2} A_b. \quad (3)$$

Namely, due to non-smooth clump surface I assume that the clump absorbs all the momentum of the wind that hits it. For an optical depth of τ_b along the radial direction of the clump the radiation exerts a force of

$$F_{\text{rad}} = A_b \frac{L}{4\pi r^2 c} (1 - e^{-\tau_b}). \quad (4)$$

I assumed above that the radiation pressure can accelerate both the wind that hits the clump, and the clump. The justification is that the radiation accelerates the wind within several stellar radii, whereas I consider the clumps at $r \gtrsim 10R_*$, where R_* is the stellar radius. These distances are outside the winds' acceleration zone and the stellar radiation is close to the photospheric radiation. Namely, I assume that the wind is optically thin while the denser clumps are cooler and have dust. The opacity of the dusty clump is $\kappa_b \approx 10 \text{ cm}^2 \text{ g}^{-1}$, while that of the cool and partially neutral wind that contains much less dust is much lower. Overall, at tens of AUs the optical depth in the clumps is much larger than in the wind. However, further out the inner clumps make the radiation redder, and for this longer wavelength band the dust opacity becomes low.

The condition on the blob acceleration to be down (in the $-r$ direction) is $F_g + F_{\text{rad}} + F_w < 0$. Using equations (2)-(4) I find this condition to read

$$1 > \frac{F_{\text{rad}} + F_w}{-F_g} \simeq \frac{v_w^2}{v_{\text{Kep}}^2} \frac{r}{R_*} \frac{r}{l_b} k_b^{-1} \times \left[\frac{L/c}{\dot{M}_w v_w} (1 - e^{-\tau_b}) + 1 \right], \quad (5)$$

where $v_{\text{Kep}} = \sqrt{GM_*/R_*}$ is the Keplerian velocity on the surface of the star.

I assume that the clump expands radially, e.g., $A_b \propto r^2$, but that its radial length l_b stays constant. I consider two limits. If the reddening of the stellar radiation by dust close to the star is significant, then the low dust opacity to this band implies that τ_b might be low. In addition, the low clump's density at large distances also reduces τ_b . In that limit I neglect the first term in the

square parenthesis of equation (5), and so the requirement on the clump's acceleration to be negative (down to the star) reads

$$\frac{r}{R_*} \lesssim \frac{v_{\text{Kep}}}{v_w} \left(\frac{l_b}{R_*} \right)^{1/2} k_b^{1/2}. \quad (6)$$

The demand on the clumps to form an extended effervescent zone is that the value of k_b be large. I emphasise again here that it is not radiation pressure that eject the clumps from the stellar surface, but rather stellar pulsation, stellar convection, and magnetic activity in the outer envelope where gravity is relatively weak.

If on the other hand radiation pressure exerts a larger outward force on the clump than that of the wind, then I approximate $(1 - e^{-\tau_b})^{1/2} \simeq 1$, and the condition reads

$$\frac{r}{R_*} \lesssim \frac{v_{\text{Kep}}}{v_w} \left(\frac{\dot{M}_w v_w}{L/c} \right)^{1/2} \left(\frac{l_b}{R_*} \right)^{1/2} k_b^{1/2}. \quad (7)$$

Since we take $\dot{M}_w v_w \simeq L/c$ (equation 1), equations (6) and (7) are practically the same for the very evolved massive stars I study here.

The conclusion is that to form an extended effervescent zone around the star the clumps should be hundreds to thousands of times denser than the average density of the wind. The extension of the effervescent zone is

$$R_{\text{eff}} \approx 6.7 \times 10^{14} \left(\frac{k_b}{1000} \right)^{1/2} \left(\frac{R_*}{2 \text{ AU}} \right) \times \left(\frac{l_b}{R_*} \right)^{1/2} \left(\frac{v_w}{v_{\text{esc}}} \right)^{-1} \text{ cm}, \quad (8)$$

where I assume that the wind is saturated in the sense that $\dot{M}_w v_w \simeq L/c$ and that the wind speed is about the escape speed from the stellar surface $v_{\text{esc}} = 2^{1/2} v_{\text{Kep}}$.

The density in the clump is

$$\rho_b \simeq 9 \times 10^{-11} \left(\frac{\dot{M}_{\text{wc}}}{4 \times 10^{-5}} \right) \left(\frac{r}{1 \text{ AU}} \right)^{-2} \times \left(\frac{v_w}{100 \text{ km s}^{-1}} \right)^{-1} \left(\frac{k_b}{1000} \right) \text{ g cm}^{-3}. \quad (9)$$

This density is more than one order of magnitude smaller than the density at the photosphere of RSG stars, ρ_p . As examples, a stellar model of zero age main sequence star of $M_{\text{ZAMS}} = 15M_\odot$ has a photospheric density of $\rho_p(1 \text{ AU}) = 5 \times 10^{-9} \text{ g cm}^{-3}$ and $\rho_p(2 \text{ AU}) = 3 \times 10^{-9} \text{ g cm}^{-3}$, at stellar radii of $R_* = 1 \text{ AU}$ and $R_* = 2 \text{ AU}$, respectively, along its evolution (I obtained these values from simulating stellar models with the open stellar evolution code MESA; Paxton et al. 2018). A stellar model of $M_{\text{ZAMS}} = 30M_\odot$ has

a photospheric density of $\rho_p(2 \text{ AU}) = 4 \times 10^{-9} \text{ g cm}^{-3}$ and $\rho_p(5 \text{ AU}) = 6 \times 10^{-10} \text{ g cm}^{-3}$, at stellar radii of $R_* = 2 \text{ AU}$ and $R_* = 5 \text{ AU}$, respectively. This implies that the star might lift such clumps above the photosphere.

4. AN EFFERVESCENT ZONE FROM A GROUP OF UNIQUE VELOCITY CLUMPS

4.1. The average density

Consider a case when the activity in the envelope of the RSG star (pulsation, convection, rotation, magnetic activity, powerful radiation) ejects bound mass, i.e., with less than the escape velocity, at a rate of

$$\dot{M}_{\text{eff}} = \beta \dot{M}_w. \quad (10)$$

Consider also that the main force on the clumps is gravity, as the other forces that we consider in section 2 play a role at very large radii where we assume that the effervescent zone is already depleted. The time it takes a clump to reach a maximum radius R_{eff} and fall back to the star is

$$t_{\text{eff}} \simeq \frac{2\pi}{2^{3/2}} \frac{R_*}{v_{\text{Kep}}} \left(\frac{R_{\text{eff}}}{R_*} \right)^{3/2}. \quad (11)$$

A wind element spends a time of $t_w(R_{\text{eff}}) \simeq R_{\text{eff}}/v_w$ in the effervescent zone. The ratio of the average density of the bound mass to that of the wind (total mass divided by total volume) in the effervescent zone is therefore

$$\begin{aligned} \frac{\bar{\rho}_{\text{eff}}}{\bar{\rho}_w} &\simeq \frac{\pi}{\sqrt{2}} \left(\frac{R_{\text{eff}}}{R_*} \right)^{1/2} \left(\frac{v_w}{v_{\text{Kep}}} \right) \beta \\ &= 17 \left(\frac{R_{\text{eff}}}{30R_*} \right)^{1/2} \left(\frac{v_w}{v_{\text{esc}}} \right) \beta, \end{aligned} \quad (12)$$

where in the second equality I scaled the wind velocity with the escape velocity from the RSG star.

Of course, many clumps will reach much smaller radii and spend much less time in the effervescent zone. On the other hand, for active RSG stars I expect $\beta > 1$. Namely, most of the gas that the envelope activity lifts around the photosphere does not reach the escape velocity. The clumps move at a lower velocity in the outer regions of the effervescent zone, so the density ratio in the outer regions of the effervescent zone is larger even. For example, 55% of its round trip the clump spends in the outer 20 percent of the effervescent zone, $0.8R_{\text{eff}}$ to R_{eff} . For the same parameters I used in scaling equation (12) the ratio of average densities in this outer region of the effervescent zone, $(\bar{\rho}_{\text{eff}}/\bar{\rho}_w)_{0.8-1} \simeq 47$.

I emphasise two points. (1) This large density ratio exists despite that the mass ejection rate into the effervescent zone is about equal to that in the wind, $\beta \simeq 1$.

(2) The derivation in this section assumes that the RSG activity brings the wind to the escape velocity, but a similar amount of mass to be close to, but below, the escape velocity. The process of acceleration takes place along several stellar radii, and therefore the derivation here are approximate. Nonetheless, equation (12) does give the general behavior of the effervescent zone.

4.2. The density profile

I consider that all clumps are ejected to radius R_{eff} . In that case the average density at each radius, but not within a distance of l_b from R_{eff} is

$$\rho_{\text{eff}}(r) \simeq 2 \frac{\dot{M}_{\text{eff}}}{4\pi r^2 v_b} \quad \text{for} \quad R_* < r < R_{\text{eff}} - l_b, \quad (13)$$

where the factor 2 comes from that each clump moves outward and fall back. As above, I neglect the forces on the clumps due to radiation and the wind, and so the velocity of the clump is

$$v_b \simeq \sqrt{\frac{2GM_*}{R_{\text{eff}}}} \sqrt{\frac{R_{\text{eff}}}{r} - 1}. \quad (14)$$

With the aid of equations (10) and (14), equation (13) becomes

$$\begin{aligned} \rho_{\text{eff}}(r) &\simeq 2 \frac{\beta \dot{M}_w}{4\pi r^2 v_{\text{esc}}} \left(\frac{R_{\text{eff}}}{R_*} \right)^{1/2} \left(\frac{R_{\text{eff}}}{r} - 1 \right)^{-1/2} \\ &= 2\beta \rho_w(r) \left(\frac{v_w}{v_{\text{esc}}} \right) \left(\frac{R_{\text{eff}}}{R_*} \right)^{1/2} \left(\frac{R_{\text{eff}}}{r} - 1 \right)^{-1/2} \\ &\quad \text{for} \quad R_* < r < R_{\text{eff}} - l_b. \end{aligned} \quad (15)$$

I note the following properties of the above density profile.

(1) For $R_{\text{eff}} \gg R_*$, as is the case in the present study, close to the star, i.e. at $r \simeq R_*$ the density of the bound gas is $\rho_{\text{eff}} \simeq 2\beta \rho_w$.

(2) For the above simple density profile case, the minimum value of the density is at $r = 0.75R_{\text{eff}}$. At that radius

$$(\rho_{\text{eff}})_{\text{min}} = \rho_{\text{eff}}(0.75R_{\text{eff}}) \simeq 19\beta \left(\frac{R_{\text{eff}}}{30R_*} \right)^{1/2} \rho_w. \quad (16)$$

This ratio increases to, e.g., 33 at $r = 0.9R_{\text{eff}}$, keeping other parameters the same.

(3) The density profile is quite flat in an extended region (equation 15). As three examples,

$$\rho_{\text{eff}} = \rho_{\text{eff}}(0.75R_{\text{eff}}) \times \begin{cases} 1.57 & \text{at } r = 0.95R_{\text{eff}} \\ 1.19 & \text{at } r = 0.55R_{\text{eff}} \\ 1.66 & \text{at } r = 0.40R_{\text{eff}}. \end{cases} \quad (17)$$

Overall, if we consider the increase in density near R_{eff} that gives the high average density in the outer regions

of the effervescent zone (equation 12 and the discussion below it), we see that the ejection at a mass rate about equal to that of the wind might mimic a short-lived wind with a mass loss rate that is tens times larger than the real mass loss rate.

5. AN EXAMPLE OF VELOCITY DISTRIBUTION

In the first paper on the effervescent zone that aimed at AGB stars (Soker 2008) I concentrated on a simple derivation of a density profile for a specific case (for more details see that paper). I assumed that the bound gas is ejected from a radius of $R_0 \approx \text{few} \times R_*$ (for the motivation to take $R_0 \approx \text{few} \times R_*$ for the extended dense zone see Soker 2008 and Dessart et al. 2017), and I took the mass ejection rate in the velocity interval v to $v + dv$ as

$$d\dot{M}_e = f\dot{M}_w \left(\frac{v}{v_{\text{esc},0}} \right)^q \frac{dv}{v_{\text{esc},0}} \quad \text{for } 0 < v < v_m, \quad (18)$$

where $v_{\text{esc},0}$ is the escape speed from R_0 and q ($-k_v$ in Soker 2008) is a constant of the model. The maximum velocity v_m is for clumps that reach the outer boundary of the effervescent zone R_{eff} , with the relation $v_m = v_{\text{esc},0} (1 - R_0/R_{\text{eff}})^{1/2}$. The total rate of unbound mass that the star ejects to the effervescence zone is

$$\begin{aligned} \dot{M}_{\text{eff}} &= \frac{f}{1+q} \left(\frac{v_m}{v_{\text{esc},0}} \right)^{1+q} \dot{M}_w \\ &= \frac{f}{1+q} \left(1 - \frac{R_0}{R_{\text{eff}}} \right)^{\frac{1+q}{2}} \dot{M}_w, \end{aligned} \quad (19)$$

From this, $f = (1+q) (1 - R_0/R_{\text{eff}})^{-(1+q)/2} \beta$, where I defined β in equation (10).

As I expect the very luminous RSG stars to lift more gas closer to the escape speed I take $q \gg 1$ (in the first paper I took low values of $q \approx 1$, and even negative values). Under the very crude assumption that each dense clump spends all the time at the maximum radius of its up and down trajectory I derived (Soker 2008) the ratio of the bound density to the escaping wind density as

$$\begin{aligned} \frac{\rho_{\text{eff}}}{\rho_w} &\approx (1+q)\beta \left(1 - \frac{R_0}{R_{\text{eff}}} \right)^{-\frac{1+q}{2}} \frac{\pi}{2} \left(\frac{v_w}{v_{\text{esc}}} \right) \left(\frac{R_0}{R_*} \right) \\ &\times \left(\frac{r}{R_*} \right)^{-1/2} \left(1 - \frac{R_0}{r} \right)^{\frac{q-1}{2}} \quad \text{for } R_0 < r < R_{\text{eff}}, \end{aligned} \quad (20)$$

where as before v_{esc} is the escape velocity from the stellar surface. I scale equation (20) to allow comparison to

equations (16) and (17)

$$\begin{aligned} \frac{\rho_{\text{eff}}}{\rho_w} &\approx 9.3 \frac{(1+q)\beta}{10} \left(\frac{v_w}{v_{\text{esc}}} \right) \left(\frac{R_0}{3R_*} \right) \left(\frac{r}{20R_*} \right)^{-1/2} \\ &\times \left[\left(1 - \frac{R_0}{R_{\text{eff}}} \right)^{-\frac{1+q}{2}} \frac{1}{1.69} \right] \\ &\times \left[\left(1 - \frac{R_0}{r} \right)^{\frac{q-1}{2}} \frac{1}{0.52} \right] \quad \text{for } R_0 < r < R_{\text{eff}}, \end{aligned} \quad (21)$$

where I normalised terms for $q = 9$, $r = (20/3)R_0 = 20R_*$, and $R_{\text{eff}} = 10R_0 = 30R_*$ (for $R_0 = 3R_*$).

Keeping all other parameters the same, the ratio in equation (21) at two other radii are $\rho_{\text{eff}}/\rho_w \approx 8.4$ and 9.6 , at $r = 5R_0 = 15R_*$ and $r = 10R_0 = R_{\text{eff}}$, respectively. Over all, the density in the outer regions of this version of the effervescent zone decreases more or less as r^{-2} , as the wind does. To increase the density in the outer regions of the effervescent zone to tens times the wind density for this distribution of clump velocities, would require taking $\beta > 1$ and/or increasing further the value of q .

6. SUMMARY AND IMPLICATIONS

I presented a phenomenological model for an extended high density zone around RSG stars at the end of their life. The basic assumption is that dense clumps, much denser than the escaping wind, move up and fall back. I term this the effervescent CSM model. The effervescent zone extends to tens of stellar radii, i.e., to $R_{\text{eff}} \approx 10 - 100 \text{ AU} \approx 10^{14} - 10^{15} \text{ cm}$ for RSG stars. Such an effervescent zone might exist only when the RSG is large, such that surface gravity is relatively weak, and the radial momentum flux of the (escaping) wind is about equal to the momentum flux of the stellar radiation (equation 1).

The effervescent CSM model assumes that during such a stellar evolutionary phase the stellar activity (rotation, convection, magnetic activity, disturbances from the vigorous core nuclear burning; see section 1) lifts large amounts of mass above the photosphere, but the stellar radiation manages to unbound only about half of that mass or less. The rest almost escapes, but falls back after reaching large radii. To fall back rather than be accelerated by radiation and the wind, the effervescent zone extends to no more than tens to about one hundred of AUs (equation 8).

I considered two phenomenological distributions of clumps' velocities (after accelerated out). In the first one (section 4), all clumps move at one velocity very close to the escape velocity. I found that the average density of the bound gas (equation 12) is tens times

larger than that of the escaping wind, in particular in the outer regions of the effervescent zone (equations 16, 17).

For example, consider a case where the outer radius of the effervescent zone is 20 times the stellar radius of a large RSG star of stellar radius $R_* = 2$ AU, i.e., $R_{\text{eff}} \simeq 20R_* \simeq 40$ AU $\simeq 6 \times 10^{14}$ cm. For the escaping wind properties as given by equation (1), which for $v_w = v_{\text{esc}}$ corresponds to an RSG star of mass $M_* = 11.3M_\odot$, the total wind mass inside $r < R_{\text{eff}}$ is $M_w(R_{\text{eff}}) \simeq 7 \times 10^{-5}M_\odot$. However, the mass of the bound gas is 14β times larger (equation 12), i.e., $M_{\text{eff}} \simeq 0.001\beta M_\odot$. However, in the very outer parts of the effervescent zone this ratio can be as large as ≈ 100 , mimicking a mass loss rate in the last year or so of $\approx 0.001 - 0.01M_\odot \text{ yr}^{-1}$. This might explain some cases of CCSNe with compact CSM, e.g., in SN 2013fs for which Yaron et al. (2017) estimated an enhanced mass loss rate of $\simeq 0.3 - 4 \times 10^{-3}M_\odot \text{ yr}^{-1}$.

Dessart et al. (2017) already considered a dense bound gas around RSG progenitors of CCSNe. In the present study I presented calculations of outflowing and inflowing gas to obtain the density profile, rather than assuming it or taking an extended stellar atmosphere. Dessart et al. (2017) estimate the mass around the progenitor of SN 2013fs to have been $\approx 0.01M_\odot$ spread over $\approx 2 \times 10^{14}$ cm. To account for this amount of mass we would require $\beta \approx 10$ in the frame of the effervescent CSM model that I studied here. To account for a compact CSM of $0.04M_\odot$ as in SN 2016bkv (Hosseinzadeh et al. 2018) or of $0.07M_\odot$ as in SN 2018cuf (Dong et al. 2021), we would require to take $\beta \simeq 10$. It is a large value, but not unreasonable in the effervescent model if the RSG experiences strong stellar activity, e.g., due to rapid rotation.

In section 5 I adopted the velocity distribution of the clumps (equation 18) from my earlier paper (Soker 2008). I followed the treatment from that paper, and derived the density profile for this clumps' velocities distribution in equations (20) and (21). This case requires values of $\beta > 1$ to achieve high densities in the outer effervescent zone.

Prentice et al. (2020) study the type IIb (envelope-stripped) SN 2018gix and argue that its CSM was non-

spherical, probably a torus, and extended to about 20 – 30 AU at explosion. They further estimate the mass in the CSM to be $\approx 0.004 - 0.014M_\odot$ and the mass loss rate from the progenitor that formed this CSM to be $\approx 0.01 - 0.05M_\odot \text{ yr}^{-1}$. If indeed the CSM is in a torus, this geometry suggests a strong binary interaction (e.g., Gofman & Soker 2019) that probably spun-up the progenitor. With rapid rotation the stellar progenitor might be able to lift a dense equatorial effervescent zone with the required mass. I therefore raise the possibility that even in these non type II CCSN the compact CSM might be an effervescent zone rather than an intensive escaping wind.

The main motivation to consider the effervescent zone in RSG stars is to remove both the requirement for fine-tuned and strong stellar activity years to months before explosion. The effervescent CSM model can exist for a long time, thousands of years and more before explosion, and the flow structure by which the gas does not reach the escape speed does not require strong activity. Moderate activity due to some extra rotation and/or moderate core activity might be sufficient.

Another effect of the effervescent zone is an extra mass transfer to a companion, if exists within and close to the effervescent zone (Soker 2008). To have a high mass transfer rate it is sufficient that the effervescent zone overfills the Roche lobe of the RSG star, such that mass transfer through the first Lagrangian point takes place (Harpaz et al. 1997; Mohamed & Podsiadlowski 2007, 2012; Chen et al. 2017; Saladino et al. 2018; Chen et al. 2020; this is also termed wind-Roche lobe overflow). Due to the high specific angular momentum of the transferred mass, it will form an accretion disk around the secondary star (if it is not a giant). In turn, the accretion disk is likely to launch two jets that will shape the CSM (e.g., Hillel et al. 2020).

ACKNOWLEDGMENTS

I thank Avishai Gilkis, Amit Kashi and an anonymous referee for useful comments. I thank Aldana Grichener for simulating stellar models. This research was supported by a grant from the Israel Science Foundation (420/16 and 769/20) and a grant from the Asher Space Research Fund at the Technion.

REFERENCES

- Boian, I. & Groh, J. H. 2020, MNRAS, 496, 1325
 Bruch, R. J., Gal-Yam, A., Schulze, S., et al. 2020, arXiv:2008.09986
 Chen, Z., Frank, A., Blackman, E. G., Nordhaus, J., & Carroll-Nellenback J. 2017, MNRAS, 468, 4465
 Chen, Z., Ivanova, N., & Carroll-Nellenback, J. 2020, ApJ, 892, 110
 Cotton, W. D., Vlemmings, W., Mennesson, B., et al. 2006, A&A, 456, 339

- Dessart, L., John Hillier, D., & Audit, E. 2017, *A&A*, 605, A83
- Diamond, P. J. & Kemball, A. J. 2003, *ApJ*, 599, 1372
- Dong, Y., Valenti, S., Bostroem, K. A., et al. 2021, arXiv:2010.09764
- Foley, R. J., Smith, N., Ganeshalingam, M., Li, W., Chornock, R., & Filippenko, A. V. 2007, *ApJL*, 657, L105
- Fonfría, J. P., Cernicharo, J., Richter, M. J., & Lacy, J. H. 2008, *ApJ*, 673, 445
- Freytag, B., Steffen, M., & Dorch, B. 2002, *Astronomische Nachrichten*, 323, 213
- Fuller, J. 2017, *MNRAS*, 470, 1642
- Fuller, J. & Ro, S. 2018, *MNRAS*, 476, 1853
- Gofman, R. A. & Soker, N. 2019, *MNRAS*, 488, 5854
- Harpaz, A., Rappaport, S., & Soker, N. 1997, *ApJ*, 487, 809
- Hillel, S., Schreier, R., & Soker, N. 2020, *ApJ*, 891, 33
- Hossein-zadeh, G., Valenti, S., McCully, C., et al. 2018, *ApJ*, 861, 63
- Humphreys, R. M., Helton, L. A., & Jones, T. J. 2007, *AJ*, 133, 2716
- Josselin, E. & Plez, B. 2007, *A&A*, 469, 671
- Kamiński, T. 2019, *A&A*, 627, A114
- Kervella, P., Lagadec, E., Montargès, M., et al. 2016, *A&A*, 585, A28
- Khoury, T., Vlemmings, W. H. T., Paladini, C., et al. 2020, *A&A*, 635, A200
- Klochkova, V. G. & Chentsov, Y. L. 2007, *Astronomy Reports*, 51, 994
- Li, A. 2003, *ApJL*, 599, L45
- Lobel, A. & Dupree, A. K. 2000, *ApJ*, 545, 454
- Lopez, B., Danchi, W. C., Bester, M., et al. 1997, *ApJ*, 488, 807
- Margutti, R., Kamble, A., Milisavljevic, D., et al. 2017, *ApJ*, 835, 140
- Margutti, R., Milisavljevic, D., Soderberg, A. M., et al. 2014, *ApJ*, 780, 21
- Mcley, L., & Soker, N. 2014, *MNRAS*, 445, 2492
- Mohamed, S., & Podsiadlowski, P. 2007, 15th European Workshop on White Dwarfs, 372, 397
- Mohamed, S., & Podsiadlowski, P. 2012, *Baltic Astronomy*, 21, 88
- Moriya, T. J., Förster, F., Yoon, S.-C., Gräfener, G., & Blinnikov, S. I., 2018, *MNRAS*, 476, 2840
- Moriya, T. J., Maeda, K., Taddia, F., Sollerman, J., Blinnikov, S. I., Sorokina, E. I. 2014, *MNRAS*, 439, 291
- Moriya, T. J., Yoon, S.-C., Gräfener, G., & Blinnikov, S. I. 2017, *MNRAS*, 469, L108
- Morozova, V., Piro, A. L., Fuller, J., & Van Dyk S. D. 2020, *ApJL*, 891, L32
- Ofek, E. O., Sullivan, M., Shaviv, N. J., et al. 2014, *ApJ*, 789, 104
- Ohnaka, K., Weigelt, G., Millour, F., et al. 2011, *A&A*, 529, A163
- Owocki, S. P., & van Marle, A. J., 2008, in *Massive Stars as Cosmic Engines*, IAU Symp 250, ed. F. Bresolin, P. A. Crowther, & J. Puls (Cambridge Univ. Press) Volume 250, p. 71-82.
- Pastorello, A., Cappellaro, E., Inserra, C., et al. 2013, *ApJ*, 767, 1
- Pastorello, A., Smartt, S. J., Mattila, S., et al. 2007, *Nature*, 447, 829
- Paxton, B., Schwab, J., Bauer, E. B., et al. 2018, *The Astrophysical Journal Supplement Series*, 234, 34.
- Planesas, P., Bachiller, R., Martin-Pintado, J., & Bujarrabal, V. 1990, *ApJ*, 351, 263
- Prentice, S. J., Maguire, K., Boian, I., et al. 2020, arXiv:2009.10509
- Quataert, E., & Shiode, J. 2012, *MNRAS*, 423, L92
- Ryde, N. & Schöier, F. L. 2001, *ApJ*, 547, 384
- Saladino, M. I., Pols, O. R., van der Helm, E., Pelupessy, I., & Portegies Zwart S. 2018, *A&A*, 618, A50
- Shiode, J. H., & Quataert, E. 2014, *ApJ*, 780, 96
- Smith, N., Miller, A., Li, W., et al. 2010, *AJ*, 139, 1451
- Soker, N. 2008, *NewA*, 13, 491
- Soker, N. & Gilkis, A. 2017, *MNRAS*, 464, 3249
- Strotjohann, N. L., Ofek, E. O., Gal-Yam, A., et al. 2021, arXiv:2010.11196
- Svirski, G., & Nakar, E. 2014, *ApJL*, 788, L14
- Tartaglia, L., Pastorello, A., Sullivan, M., et al. 2016, *MNRAS*, 459, 1039
- van Marle, A. J., Owocki, S. P., & Shaviv, N. J. 2009, *MNRAS*, 394, 595
- Vlemmings, W. H. T., Diamond, P. J., & van Langevelde, H. J. 2002, *A&A*, 394, 589
- Wood, B. E. & Karovska, M. 2006, *ApJ*, 649, 410
- Yaron, O., Perley, D. A., Gal-Yam, A., et al. 2017, *Nature Physics*, 13, 510